Transition Modes in Ising Networks: An Approximate Theory for Macromolecular Recognition

Sean Keating and Enrico Di Cera
Department of Biochemistry and Molecular Biophysics, Washington University School of Medicine, St. Louis, Missouri 63110 USA

ABSTRACT For a statistical lattice, or Ising network, composed of N identical units existing in two possible states, 0 and 1, and interacting according to a given geometry, a set of values can be found for the mean free energy of the 0→1 transition of a single unit. Each value defines a transition mode in an ensemble of $\nu_N = 3^N - 2^N$ possible values and reflects the role played by intermediate states in shaping the energetics of the system as a whole. The distribution of transition modes has a number of intriguing properties. Some of them apply quite generally to any Ising network, regardless of its dimension, while others are specific for each interaction geometry and dimensional embedding and bear on fundamental aspects of analytical number theory. The landscape of transition modes encapsulates all of the important thermodynamic properties of the network. The free energy terms defining the partition function of the system can be derived from the modes by simple transformations. Classical mean-field expressions can be obtained from consideration of the properties of transition modes in a rather straightforward way. The results obtained in the analysis of the transition mode distributions have been used to develop an approximate treatment of the problem of macromolecular recognition. This phenomen is modeled as a cooperative process that involves a number of recognition subsites across an interface generated by the binding of two macromolecular components. The distribution of allowed binding free energies for the system is shown to be a superposition of Gaussian terms with mean and variance determined a priori by the theory. Application to the analysis of the biologically relevant interaction of thrombin with hirudin has provided some useful information on basic aspects of the interaction, such as the number of recognition subsites involved and the energy balance for binding and cooperative coupling among them. Our results agree quite well with information derived independently from analysis of the crystal structure of the thrombin-hirudin complex.

1. INTRODUCTION

A number of important properties of biological macromolecules can be approached conveniently in terms of lattice statistics (1). Processes such as folding and ligand-induced conformational transitions often entail cooperative transitions involving numerous subsystems, such as microdomains or binding sites (2, 3). Likewise macromolecular recognition, i.e., the process that allows proteins to interact with small ligands, other proteins, and DNA molecules, can be seen to arise from the contribution of several individual subsites that give rise to the macroscopic energetics measured experimentally. In all of these processes one seeks to capture the essential features of the system under consideration by means of an approximate treatment, which serves as a starting point for more elaborate descriptions. The approximate approach is often bound to be phenomenological rather than structural, but useful information is nonetheless extracted from an analysis of experimental data.

The ferromagnetic spin lattice (4), or Ising problem, represents the "ideal gas" model of cooperative transitions and has long provided a paradigm for processes where the enormous number of possible configurations of a system is drastically altered by interactions among its constituent parts. The reduction of the number of "intermediate" states in the transition of the system from one state to another is in fact the mark of cooperative phenomena. The reduction itself may appear as a simplification in the problem of enumerating all possible states to be taken into account, but the price to be paid for this apparent simplification is quite high and stems from the "uncertainty" of uniquely defining a mechanism for the overall behavior of the system. This fact is readily appreciated in the experimental analysis of these processes, since detection of intermediate states is a very difficult task and, at the same time, is recognized as a *conditio sine qua non* for the formulation of the rules of interaction of constituent domains or sites of a protein that bring about its folding (5) or cooperative binding (6) properties. Even from the theoretical point of view it is always important to know exactly what distribution of intermediates is to be expected for any given interaction network among the constituent parts of a system, because this information is critical to the formulation of the partition function. The difficulty of solving the partition function for an Ising spin model in arbitrary dimensions stems exactly from the difficulty of finding a recursive relation or algorithm to enumerate all possible intermediates of the system (7, 8). Since all information is stored in the intermediates, the question arises as to what analytical methods may effectively be used in decoupling the code for cooperative transitions that translates into the macroscopic behavior accessible to experimental measurements. It is clear that one should look for an approach focused on the thermodynamic properties of each constituent unit of the system. Site-specific thermodynamics provides a theory for understanding how macroscopic, global cooperative behavior arises from microscopic, local interaction patterns (9). The extraordinary complexity of site-specific effects and their unique

Received for publication 28 January 1993 and in final form 15 March 1993.
Address reprint requests to Dr. Enrico Di Cera.

0006-3495/93/07/253/17 $2.00

regulatory features make the analysis of the theory in its general formulation quite elaborate and limit its application in the "exact" form to some very special cases. Hence, the need for simplified mechanistic treatments of site-specific effects in biological macromolecules is recognized as a timely and important issue (10, 11).

In this paper we apply some basic concepts of the theory of site-specific effects to the analysis of statistical mechanical lattice models. The goal is to define a new area of investigation where the methodologies of site-specific thermodynamics merge with the fundamental results of lattice statistics. This should provide new insight into the problem of cooperative transitions and how intermediate states contribute to the overall energetics of the system. Previous studies of the combinatorics of Ising networks have relied heavily on the use of matrix algebra, sequence-generating functions, or conditional probabilities (7, 8, 12–14). Likewise, the pioneering work of Scheraga on the site-specific properties of Ising networks has been based on the Zimm-Bragg formalism and focused on the specific problem of helix-coil transitions (15). Our approach is somewhat different, insofar as it seeks to capture some essential properties of Ising networks using the distribution of "transition modes" that shape the free energy landscape of the lattice. The properties of this distribution, which encapsulates all of the important quantities of the network, are quite intriguing and are particularly useful in the systematic analysis of the global and site-specific behavior of the lattice. The analysis presented here stems from the broader perspective of the general thermodynamic approach to site-specific energetics (9) and the properties of transition free energies that can be defined for any system in a model-independent way (16). Some of the results to be described in this work apply quite generally to any Ising model, regardless of its dimension, while other results might be used to explore new ways of dealing with the combinatorics involved in the formulation of the partition function of Ising networks in any dimension. A practical application of the concepts to be dealt with in this work is given in section 8, where we develop an approximate theory for the problem of macromolecular recognition. The approximate treatment proposed here should serve as a simple conceptual framework and as a starting point for more detailed molecular analysis.

2. THE CONCEPT OF TRANSITION MODE

Let us start with the definition of an Ising network as a statistical mechanical lattice model containing N identical units. Each unit is assumed to exist in two states, to be designated henceforth by 0 and 1, consistent with the classical treatment of ferromagnetic spin lattices (1, 4). The concepts to be dealt with in this paper are independent of the specific nature of the two states, as well as of the driving force responsible for the 0→1 transition. However, for the sake of clarity and without loss of generality, one can see these states as two different conformational states of the constituent parts of a macromolecular system, say a microdomain that can exist in the folded (1) or unfolded (0) conformation (2, 5). If the temperature of the heat bath provides the driving force for the transition, the lattice as a whole can be treated as a canonical ensemble. Alternatively, the 0→1 transition may be seen to arise as a result of binding of a ligand to a specific site of the macromolecule, with states 0 and 1 denoting the free and bound forms. In this case the driving force for the transition is the chemical potential of the ligand, and the lattice as a whole can be modeled as a grand canonical ensemble. Other systems of physical and chemical interest, such as neural networks (17) or molecular quasi-species (18), can be modeled using the same conceptual framework of N units existing in two alternative states, so that it seems appropriate in what follows to cast our treatment in a rather general form instead of limiting ourselves to the analysis of a specific statistical ensemble.

For a system of N units existing in two states there are 2^N possible configurations, each of which can be represented as a N-dimensional vector of the form (11, 19)

$$[\sigma] = [\theta_1, \theta_2, \ldots, \theta_j, \ldots, \theta_N] \qquad (2.1)$$

where $\theta_j = 0,1$ is the state of the jth unit in the network. Each configuration is characterized by a specific energy level specified by the intrinsic energy levels of states 0 and 1, as well as by the interaction network among the units. If the configuration with all units in state 0 is taken as a reference, then a total of $2^N - 1$ independent free energy terms characterize the network, each corresponding to the work spent in the transition from the reference configuration to any one of the remaining $2^N - 1$ configurations. Knowledge of this free energy set completely and uniquely defines the properties of the network under consideration (9, 11). This free energy set is, however, a small subset of a much larger set of free energy values, the properties of which are quite intriguing and provide useful details on the statistical properties of the network and its intermediates. Assume we ask the rather basic question: What is the average free energy spent by one unit in the 0→1 transition? The magnitude of this free energy change clearly depends on the intrinsic properties of the network. Consider the Ising networks depicted in Fig. 1. The possible configurations are denoted by vertices and labeled according to Eq. 2.1. For $N = 1$ the free energy spent per unit in the 0→1 transition is given by the difference between the energy of states 1 and 0. For $N = 2$, on the other hand, the free energy of transition is not uniquely specified. The transition 00→01 or 00→10 provides a possible value. The transition 10→11 or 01→11 provides another value. Finally, the transition 00→11 defines a free energy change for switching two units to state 1, and when this value is divided by two, it also represents a measure of the mean free energy change spent per unit in the 0→1 transition. Not all of these values need be the same, unless one deals of course with the rather uninteresting case of the absence of interactions between the units. In the case of $N = 3$ the situation is even more complex. There are transitions of the type 000→001, 001→011, and 011→111 that involve one unit at a time, transitions of the type 000→011 and 001→111 that

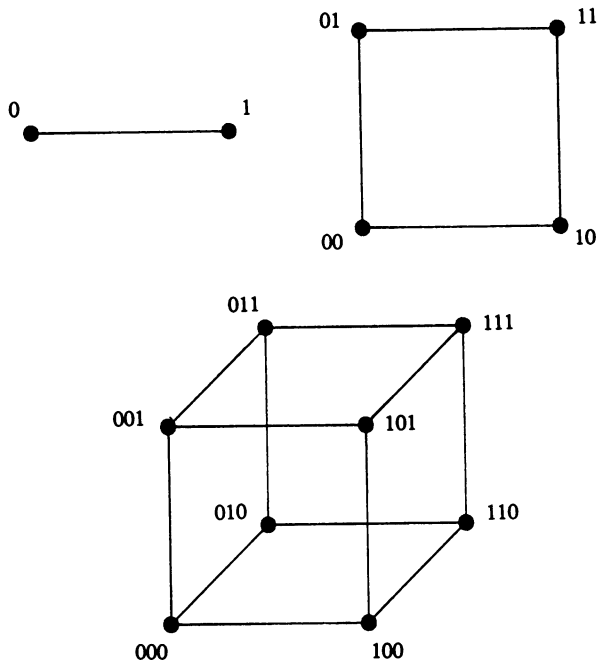

FIGURE 1 Transition diagrams for Ising networks composed of 1, 2, or 3 units. Each dot depicts a possible configuration of the system, and an edge denotes a transition between two configurations. The number of possible configurations is 2^N, and each one is labeled by a sequence of binary digits reflecting the state of the individual units. The Hamming distance separating any two configurations is obtained from the diagrams as the number of edges bridging them.

involve two units, and finally the transition 000→111, which involves all three units. One sees by inspection that for arbitrary N there are transitions involving $j = 1, 2, \ldots, N$ units, each providing in principle a different value for the mean free energy change spent per unit in the 0→1 transition. We know from information theory that in a network such as any of those depicted in Fig. 1, or for arbitrary N, each configuration can be labeled as in Eq. 2.1. Given any two configurations, $[\sigma]$ and $[\sigma']$, the number of digits that one needs to change in $[\sigma']$ to obtain $[\sigma]$ is the "Hamming distance," $H_{\sigma\sigma'}$, between $[\sigma]$ and $[\sigma']$ (19). Hence, the mean free energy spent per unit in the 0→1 transition, $\Delta G_m(\sigma, \sigma')$, is given by

$$\Delta G_m(\sigma, \sigma') = H^{-1}_{\sigma\sigma'} \Delta G_{\sigma\sigma'} \qquad (2.2)$$

Given any two configurations in the network, $[\sigma]$ and $[\sigma']$, such that $[\sigma']$ can be obtained from $[\sigma]$ by switching n units from 0 to 1, the value of $\Delta G_m(\sigma, \sigma')$ is nothing but the free energy change for the $[\sigma] \rightarrow [\sigma']$ transition divided by n, i.e., the Hamming distance $H_{\sigma\sigma'}$ between $[\sigma]$ and $[\sigma']$.

The importance of defining a free energy set given by Eq. 2.2 stems from the fact that these values depend on all possible configurations of the network and therefore reflect the properties of the intermediate states that shape the cooperative behavior of the system as a whole. The transition free energy mode, or simply *transition mode*, as defined in Eq. 2.2 is a sort of local "intensive" property of the system that labels the energetics of the elementary transition in a site-specific fashion (9). A simple and quite instructive way of thinking of the ensemble of transition mode values is a "dynamic" analogue constructed by taking a walk in the network of 2^N possible configurations, starting from any configuration $[\sigma]$ and making elementary steps of unit Hamming distance by switching one unit in state 0 to state 1 at a time. The total energy spent in realizing a particular trajectory from $[\sigma]$ to $[\sigma']$ is given by the free energy change $\Delta G_{\sigma\sigma'}$. Clearly, detailed balancing makes the result independent of the particular trajectory. The free energy change $\Delta G_{\sigma\sigma'}$, divided by the number of steps, gives the transition mode value for the trajectory, provided each step is linked to the 0→1 transition of one unit. The possible trajectory end points for the simple case of $N = 3$ are depicted in Fig. 2. When all possible transitions from $[\sigma]$ to $[\sigma']$ are considered, a distribution of transition mode values is obtained. This distribution reflects the energetic landscape of the network under consideration and the contribution of all configurations or intermediates to the macroscopic behavior of the system.

With this conceptual framework in mind we now proceed to explore the properties of the distribution of transition mode values for Ising networks of interest. To approach this problem in a rigorous and systematic way we borrow the concept of *contraction domain* from site-specific thermodynamics (9). Essentially, a transition mode is the mean free energy of 0→1 switching when the state of up to $N - 1$ units is held

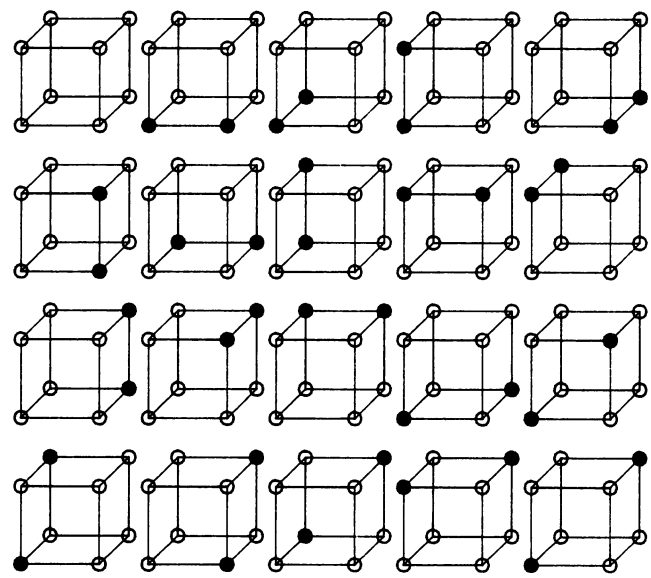

FIGURE 2 Transition diagrams for $N = 3$. Each vertex of the cube (○) corresponds to a configuration labeled as in Fig. 1. The cube at the top left corner represents the cube in Fig. 1. Filled circles depict the two configurations of interest, $[\sigma]$ and $[\sigma']$. A transition mode is the free energy spent in the transition between the two configurations in the cube, divided by their Hamming distance, $H_{\sigma\sigma'}$, which is the number of edges separating them. The number of different transition modes is $\nu_3 = 3^3 - 2^3 = 19$. Twelve modes are derived from a Hamming distance of 1, six from a Hamming distance of 2, and one from a Hamming distance of 3.

fixed. The operation of fixing M, $0 \leq M \leq N - 1$, units in a given state is referred to as a *contraction*. The set of units in the fixed state will be referred to as the *contraction domain*, and the unconstrained units constitute the *free domain*. Among the M units in the contraction domain, a number j, $0 \leq j \leq M$, may be fixed in state 1. The total number of distinct contractions, and hence transition modes, that can be generated in this way is evidently

$$\nu_N = 3^N - 2^N \tag{2.3}$$

To see this, note that the number of ways of selecting the M contracted units is given by the binomial coefficient $C_{N,M} = N!/(N - M)!\,M!$, and likewise the number of ways of selecting the j units in state 1 is $C_{M,j} = M!/(M - j)!\,j!$. *Hence the value of* N is given by the double sum over M and j

$$\nu_N = \sum_{M=0}^{N-1} \sum_{j=0}^{M} C_{N,M} C_{M,j} = 3^N - 2^N \tag{2.4}$$

Alternatively one can observe that each of the N units has three possible states: contracted in state 0, contracted in state 1, and free, giving 3^N possibilities in all, of which the 2^N where all N units are contracted (in either state 0 or 1) must be eliminated. In order to characterize the thermodynamic properties of the free domain we note that a transition mode can obviously be defined for any subsystem where the number of free units is $N - M$. Consider an arbitrary configuration with M units in the contraction domain, j of which are in state 1, while the remaining $N - M$ units in the free domains are all in state 0. Let $[\tau]$ be the label for the vector associated with the configuration of the contracted units. Then, ${}^{[\tau]}\Delta G_m(N, M, j)$ is the transition mode associated with $[\tau]$. We know that this free energy is the difference between the intrinsic energy level of the configuration where all units in the free domain are in state 1 and the intrinsic energy level of the configuration where all units in the free domain are in state 0, divided by $N - M$. For a fixed value of M and j, there are as many as $C_{N,M}C_{M,j}$ possible values of ${}^{[\tau]}\Delta G_m(N, M, j)$. We are interested in the distribution of $\Delta G_m(N, M, J)$ values in the space of the N possible contractions on the lattice. Our goal is to determine the possible values of the transition modes and their degeneracy, i.e., how many of the contractions contribute to each value. For a system where all units are different and interact differently, ν_N different values, each with a weight of 1, can be expected in principle. The question to be addressed here is what kind of distributions can be expected for Ising networks on which constraints have been placed in the form discussed at the beginning of this section.

3. GENERAL RESULTS

We begin by observing that if all units are equivalent, then each transition mode has an intrinsic weighting or degeneracy of

$$w(N, M, j) = C_{N,M} C_{M,j} \tag{3.1}$$

Without loss of generality, intrinsic energy levels of 0 and ϵ are assigned to states 0 and 1, respectively. We will say that two units *contact* one another when they are spatially located in such a way that there is a possible interaction between them, and we suppose that each site contacts r other sites, where r may be thought of as the range of the interaction or the *connectivity* of the network. At this stage we make no assumption on the dimensionality of the network wherein the units are embedded, since the results we are going to describe in this section apply quite generally to any Ising network for which r is specified. We choose the interaction potential such that two units in contact in different states interact and contribute an energy J, while units in contact in the same state contribute zero. Except for a shift in energy, this is the usual rule by which interactions are assigned in ferromagnetic spin models (1, 4). Using the above definition we introduce two parameters, i.e., the equilibrium constant for the $0 \rightarrow 1$ transition in an *isolated* unit

$$K = \exp(-\epsilon/k_B T) \tag{3.2}$$

where k_B is the Boltzmann constant and T the absolute temperature, and the interaction constant for a 01 pair of interacting units

$$\omega = \exp(-J/k_B T) \tag{3.3}$$

It is clear that the intrinsic energy level of the configuration where all units are in state 0 is exactly zero, so that this configuration can be used as a reference for the remaining $2^N - 1$ without rescaling the energy values. The sign of J defines the nature of cooperativity, positive ($J > 0$) or negative ($J < 0$), for the system (3). In the case of positive cooperativity the intermediate configurations with units in state 0 and 1 are depressed since $\omega < 1$. The opposite effect is seen in systems where $J < 0$.

Consider an arbitrary disposition of the units in the contraction domain, with all other units in the free domain in state 0. The intrinsic energy of this configuration of N units, relative to the reference, is assigned quite simply by counting the number of units in state 1 and the number of 01 pairs. Since each unit in state 1 contributes ϵ to the energy, and each 01 pair contributes J, a given configuration with M units in the contraction domain and $N - M$ units in state 0 in the free domain is characterized by an intrinsic energy level

$$E_0(N, M, j) = j\epsilon + \{\chi_0(N, M, j) + \psi(N, M, j)\}J \tag{3.4}$$

Here $\chi_0(N, M, j)$ is the number of 01 pairs across the boundary between the free and contraction domains, and the subfix zero denotes the fact that all units in the free domain are in state 0. The coefficient $\psi(N, M, j)$, on the other hand, reflects the number of 01 pairs inside the contraction domain. We now switch all units in the free domain to state 1 and compute

a new intrinsic energy level as follows:

$$E_1(N, M, j) = (N - M + j)\epsilon + \{\chi_1(N, M, j) + \psi(N, M, j)\}J \quad (3.5)$$

where $\chi_1(N, M, j)$ now denotes the number of 01 pairs across the boundary between the free and contraction domains when all units in the free domain are in state 1. The free energy change per unit in switching from state 0 to 1 is given by the expression

$$\Delta G_m(N, M, j) = \epsilon + (N - M)^{-1}\{\chi_1(N, M, j) - \chi_0(N, M, j)\}J \quad (3.6)$$

This is the transition mode of interest and, evidently, is independent of $\psi(N, M, j)$. In the special case where $M = 0$, there is no contraction domain, and Eq. 3.6 gives the mean free energy change per unit in switching from the reference configuration to that where all units are in state 1. This transition mode is quite important in practical applications since it is the one readily accessible to experimental measurements. In fact, since this transition mode is simply the work done in fully switching the system from one limiting configuration to the other, divided by the number of units, it represents the amount of energy per unit that should be supplied to the system to make these two limiting configurations equally populated. Specifically, this transition mode provides the mean free energy of unfolding in folding transitions (2), or the mean free energy of binding in grand canonical ensembles (16, 20), and will be referred to in our description as the *standard transition mode*:

$$\Delta G_m^\circ = \epsilon = -k_B T \ln K \quad (3.7)$$

solely to indicate that it reflects the properties of a standard state where the size of the contraction domain is zero.

Since a unit in state 1 interacts only with a unit in state 0, and vice versa, the sum of the possible 01 pairs $\chi_1(N, M, j) + \chi_0(N, M, j)$ is just the total number, $\chi_{tot}(N, M)$, of physical contacts between the domains. Hence,

$$\chi_1(N, M, j) + \chi_0(N, M, j) = \chi_{tot}(N, M) \quad (3.8)$$

This observation allows us to prove the following theorem, which holds quite generally for any Ising network, regardless of its dimensionality.

THEOREM: *The distribution of $\Delta G_m(N, M, j)$ values for an Ising network of N units is the sum of subdistributions symmetric about the standard transition mode ΔG_m° and itself possesses this symmetry.*

To prove this theorem let us introduce the *dual* domain, defined as that obtained from the contraction domain by switching the state of all the contracted units. All those in state 1 switch to state 0 and vice versa. Note that this leaves M unchanged but results in the replacement $j \to M - j$. We also have the conservation property, analogous to Eq. 3.8, that the sum of the possible 01 pairs χ_0 and χ_1 for a given contraction domain and its dual is just the total number of interdomain contacts, i.e.,

$$\chi_0(N, M, j) + \chi_0(N, M, M - j) = \chi_{tot}(N, M) \quad (3.9a)$$

$$\chi_1(N, M, j) + \chi_1(N, M, M - j) = \chi_{tot}(N, M) \quad (3.9b)$$

Using Eqs. 3.6 and 3.7 we can derive the sum of the transition modes for any contraction domain and its dual as follows:

$$\Delta G_m(N, M, j) + \Delta G_m(N, M, M - j) = 2\Delta G_m^\circ + (N - M)^{-1}\{\chi_1(N, M, j) + \chi_1(N, M, M - j) - \chi_0(N, M, j) - \chi_0(N, M, M - j)\}J \quad (3.10)$$

and from Eq. 3.9 one has

$$\Delta G_m(N, M, j) + \Delta G_m(N, M, M - j) = 2\Delta G_m^\circ \quad (3.11)$$

Hence, the transition modes relative to a given contraction domain and its dual are equidistant from the standard transition mode. Furthermore, since

$$w(N, M, j) = C_{N,M}C_{M,j} = C_{N,M}C_{M,M-j} = w(N, M, M - j) \quad (3.12)$$

the intrinsic weighting of any contraction, and hence the degeneracy of the transition mode associated with it, is equal to that of its dual. Equations 3.11 and 3.12 demonstrate that, for M fixed, the components in the distribution of transition modes generated by changing j occur in pairs symmetrically disposed about the standard transition mode ΔG_m°, which provides a center of symmetry (21). The self-dual contraction $M = 0$ also obeys this rule as a special case. Thus the subdistribution for any given M is symmetric about ΔG_m°, and of course the overall distribution of transition modes, which is the sum of these subdistributions, also possesses this symmetry; hence the theorem. Note that this theorem also applies to an Ising network of arbitrarily or randomly connected units. In fact, the proof does not involve the connectivity of the network and is therefore independent of whether the units are equivalent (i.e., r is the same for all units) or not. In the case where all units are equivalent, it is possible to analyze the mode distribution in more detail as follows.

The range of each subdistribution for fixed M can be determined in a straightforward way by rewriting Eq. 3.6 as follows:

$$\Delta G_m(N, M, j) = \Delta G_m^\circ - (N - M)^{-1} \times \{\chi_{tot}(N, M) - 2\chi_1(N, M, j)\}J \quad (3.13)$$

The number of 01 pairs $\chi_1(N, M, j)$ varies from 0 for $j = M$ to $\chi_{tot}(M, N)$ for $j = 0$, so the limits for the transition modes

for a given value of M are clearly

$$^{\pm}\Delta G_m(N, M, j) = \Delta G_m^\circ \pm (N - M)^{-1}\chi_{tot}(N, M)J \quad (3.14)$$

and we therefore require the maximum value of $\chi_{tot}(N, M)$ for a given M. Suppose that $M \leq N/r$, where we recall that r is the connectivity of the network. Then there is a disposition of the contracted sites such that there is no contact within the contraction domain, in which case

$$\chi_{tot}(N, M) = rM \quad (3.15)$$

Hence,

$$^{\pm}\Delta G_m(N, M, j) = \Delta G_m^\circ \pm M(N - M)^{-1}rJ \quad \text{for} \quad M \leq N/r \quad (3.16)$$

For $M \geq N/r$ there is a disposition of the contracted sites such that there is no contact within the free domain, so the maximum value of $\chi_{tot}(N, M)$ is given by

$$\chi_{tot}(N, M) = r(N - M) \quad (3.17)$$

Hence,

$$^{\pm}\Delta G_m(N, M, j) = \Delta G_m^\circ \pm rJ \quad \text{for} \quad M \geq N/r \quad (3.18)$$

and the transition modes of the overall distribution satisfy

$$\Delta G_m^\circ - rJ \leq \Delta G_m(N, M, j) \leq \Delta G_m^\circ + rJ \quad (3.19)$$

As already noted, the overall distribution of transition modes can be regarded as the superposition of N subdistributions with $M = 0, 1, \ldots, N - 1$. Since $\chi_{tot}(N, M) - 2\chi_1(N, M, j)$ in Eq. 3.13 must be an integer, each subdistribution has a characteristic spacing of $J/(N - M)$, in the sense that this is the minimum possible distance between two transition modes within the subdistribution. The set of values that $\chi_{tot}(N, M) - 2\chi_1(N, M, j)$ can actually take on depends on the details of the model, specifically the value of r and the dimensional embedding, i.e., whether we are dealing with one-, two-, or n-dimensional Ising networks. Once these variables are known, the transition modes are fully defined. However, the degeneracy arising from the number of ways of realizing each transition mode will in general be a formidable combinatorial problem.

We have pointed out in the Introduction that the free energy set associated with the $2^N - 1$ independent transitions from the reference configurations to the remaining ones is a subset of the distribution of transition modes. In fact, the free energy difference between any configuration and the reference configuration with all units in state 0 can be derived from the transition modes in a straightforward way by imposing $j = 0$ and multiplying the resulting value of $\Delta G_m(N, M, 0)$, obtained for a given value of M and disposition of units in the contraction domain, by $N - M$. These values enter the definition of the partition function of the network, and therefore by studying the properties of the transition modes we should be able to understand some basic properties of the coefficients of the partition function of an Ising network, as will be shown in section 7. In this section we have established some general features of the mode distribution for Ising networks. It should be mentioned that if an asymmetric form for unit-unit interaction is used, then a weaker form of the symmetry theorem, requiring that the units be equivalent, holds. The proof is similar, but requires in addition Eq. 5.1, thus introducing the restriction. For example, if we suppose that only units in state 1 interact in an Ising network of equivalent units, as might be appropriate for a lattice gas model (1), then the transition mode distribution $P(x)$ is shifted along the x-axis and compressed by a factor of 2 but retains its symmetry features as implied by the theorem. In an Ising network of nonequivalent units, say a linear Ising chain, the mode distribution is symmetric with the symmetric (ferromagnetic) interaction but is otherwise asymmetric. It is also interesting to note that the general features outlined in this section are independent of the dimensionality of the network, since the analysis was based entirely on combinatorial and counting arguments. In the following sections we analyze in detail the properties of two specific Ising models that are of particular relevance in practical applications.

4. FULLY CONNECTED ISING NETWORK

Consider an Ising network where each unit is in contact with every other unit, so that the connectivity r is given by $r = N - 1$. This interaction geometry, which we refer to as the fully connected Ising model, is the simplest case of interest because the quantities $\chi_{tot}(N, M)$ and $\chi_1(N, M, j)$ are independent of the disposition of the contracted units and are uniquely defined once N, M, and j are specified. In fact, it is easy to see that

$$\chi_{tot}(N, M) = M(N - M) \quad (4.1a)$$

$$\chi_1(N, M, j) = (M - j)(N - M) \quad (4.1b)$$

for all contractions. Substitution of Eq. 4.1 into Eq. 3.13 yields

$$\Delta G_m(N, M, j) = \Delta G_m^\circ + (M - 2j)J = \Delta G_m^\circ + nJ \quad (4.2)$$

where $n = M - 2j$ varies from $-(N - 1)$ to $(N - 1)$, since $M = 0, 1, \ldots, N - 1$ and $j = 0, 1, \ldots, M$. Hence, the transition modes for this model are uniformly distributed in the range $\pm(N - 1)J$, with a spacing of J. For fixed M, the distribution is symmetric around $j = M/2$, as implied by the theorem in section 3, has a spacing of $2J$, and follows the binomial $C_{M,j}$. For N large, M is also large, and the binomial distribution $C_{M,j}$ goes into a Gaussian with mean $M/2$ and variance $M/4$, as implied by the De Moivre–Laplace theorem (22). Incidentally, the Gaussian approximation is remarkably good, even for values of N as small as 6 (22). Hence, each subdistribution for fixed M can be approximated well by a Gaussian distribution with mean and variance given by

$$\mu(N, M) = \Delta G_m^\circ \quad (4.3a)$$

$$\sigma^2(N, M) = MJ^2 \quad (4.3b)$$

Notice that the mean is independent of M, while the variance

grows linearly with the size of the contraction domain, independently of N. This result can be seen as the exact parallel of Brownian motion in one dimension (23) around the origin $x = \Delta G_m^\circ$, where M plays the role of time and the diffusion coefficient D is proportional to J^2. In the absence of interactions $J = 0$, and no diffusion is observed around the standard transition mode. In this case the overall distribution is a delta function peaked at $x = \Delta G_m^\circ$. For finite J, and regardless of whether interactions stabilize ($J < 0$) or destabilize ($J > 0$) units in contact, the distribution of transition modes spreads out with increasing M under the effect of a "drift" provided by the interaction energy J. The further away two configurations $[\sigma]$ and $[\sigma']$ are from each other, the more likely the transition mode is to be close to the standard transition mode ΔG_m°. The greater the Hamming distance $H = N - M$ between two configurations, the smaller is the variance of the distribution of transition modes associated with it. The variance of the subdistributions obtained for $N = 20$ is shown in Fig. 3 as a function of M. A straight line is observed as predicted by Eq. 4.3b, with a slope equal to J^2.

The intrinsic weight of each subdistribution goes as 2^M. The overall distribution of transition modes is simply the sum of all subdistributions obtained for fixed M, each weighted according to 2^M, times the number of ways of fixing M units among N, $C_{N,M}$. Some overlap exists among the subdistributions since, as implied by Eq. 4.2, all values of M and j such that $M - 2j = n =$ constant contribute to the same mode.

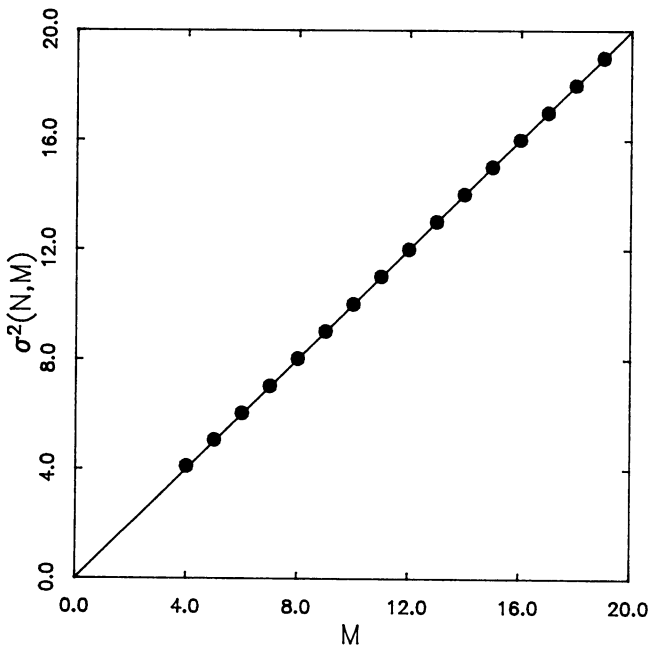

FIGURE 3 Dependence of the variance of the subdistributions of transition modes for fixed M as a function of M, in the case of the fully connected Ising network ($r = N - 1$) for $N = 20$ and $J = 1$. The theory predicts each subdistribution to be approximately a Gaussian with mean and variance given in Eq. 4.3, and the continuous line confirms the validity of this prediction.

This constraint acts as a filter for the entire set of combinations that generates the ensemble of N transition modes. The degeneracy, $P(n)$, of a given mode is therefore given by

$$P(n) = \sum_{M=0}^{N-1} \sum_{j=0}^{M} C_{N,M} C_{M,j} \delta_{mn} \tag{4.4}$$

where the Kronecker delta δ_{mn} filters out all values of $m = M - 2j$ not equal to the prescribed value of n. The analytical form of $P(n)$ can be found by introducing the integral representation of δ_{mn} as follows (24):

$$\delta_{mn} = \frac{1}{2\pi} \int_0^{2\pi} \exp\{i(n - m)\varphi\}\, d\varphi \tag{4.5}$$

Since the double sum in Eq. 4.4 exists and is finite, we can interchange it with the integral above to obtain

$$P(n) = \frac{1}{2\pi} \int_0^{2\pi} \exp(in\varphi) \times \sum_{M=0}^{N-1} \sum_{j=0}^{M} C_{N,M} C_{M,j} \exp\{i(2j - M)\varphi\}\, d\varphi \tag{4.6}$$

Elementary transformations involving the double sum lead to

$$P(n) = \frac{1}{2\pi} \int_0^{2\pi} \exp(in\varphi) \times \{(1 + 2\cos\varphi)^N - 2^N \cos^N\varphi\}\, d\varphi \tag{4.7}$$

and due to the symmetry of the integrand one also has

$$P(n) = \frac{1}{\pi} \int_0^{\pi} \exp(in\varphi) \times \{(1 + 2\cos\varphi)^N - 2^N \cos^N\varphi\}\, d\varphi \tag{4.8}$$

In the limit of large N the expression in braces has a dominant peak with maximum 3^N at $\delta = 0$. The value of the maximum is the expected value of ν_N in the same limit. The Taylor expansion around this point yields

$$(1 + 2\cos\varphi)^N - 2^N \cos^N\varphi \approx 3^N(1 - \varphi^2/3)^N \approx 3^N \exp(-N\varphi^2/3) \tag{4.9}$$

In this limit the upper bound of the integral can be extended to ∞, and substitution into of Eq. 4.9 into Eq. 4.8 yields

$$P(n) = (3^N/\pi) \int_0^{\infty} \exp(in\varphi) \exp(-N\varphi^2/3)\, d\varphi = 3^N(4\pi N/3)^{-1/2} \exp(-3n^2/4N) \tag{4.10}$$

The distribution $P(n)$ of n values is the Fourier transform of a Gaussian distribution and is therefore itself a Gaussian,

with a mean of zero and a variance equal to $2N/3$. The overall distribution of transition modes for the fully connected Ising network is a Gaussian with mean and variance equal to

$$\mu(N) = \Delta G_m^\circ \tag{4.11a}$$

$$\sigma^2(N) = 2NJ^2/3 \tag{4.11b}$$

This distribution can be exhaustively calculated with a computer, and Fig. 4 shows the results of such a calculation for $N = 20$, together with the theoretical Gaussian with parameters given by Eq. 4.11. The distribution spans the range $\Delta G_m^\circ - (N - 1)J$ to $\Delta G_m^\circ + (N - 1)J$ as implied by Eq. 3.19, with the $2N - 1$ distinct modes uniformly distributed in that interval with a spacing of J. A substantial agreement is seen between the actual distribution of transition mode values and that predicted by our analysis.

5. ISING RING NETWORK

As a second example of an Ising model we consider a ring of sites in one dimension, where each site interacts only with its nearest neighbors. Obviously $r = 2$ in this case, and from the general theory we know that the transition mode distribution will be symmetric and span the range from $\Delta G_m^\circ - 2J$ to $\Delta G_m^\circ + 2J$. As in the previous example, in order to determine the values for the transition modes we must find

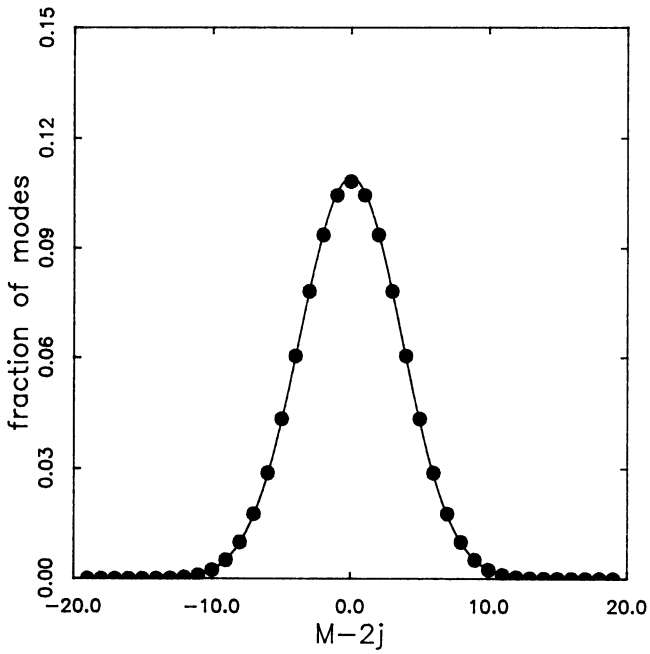

FIGURE 4 Distribution of transition modes for the fully connected Ising network ($r = N - 1$) for $N = 20$. The degeneracy of each mode has been normalized by $\nu_N = 3^N - 2^N$ to yield the probability of occurrence (or fraction of modes) shown. The values are plotted versus $M - 2j$ according to the definition given in Eq. 4.2, with values of $\Delta G_m^\circ = 0$ and $J = 1$ used for the sake of simplicity. The continuous line depicts a Gaussian distribution with a mean of zero and a variance equal to $2N/3$. This is the limiting distribution predicted theoretically in section 4 (see Eq. 4.11).

the possible values of $\chi_{tot}(N, M)$ and $\chi_1(N, M, j)$ for all contraction domains. The possible values for $\chi_{tot}(N, M)$ are subject to the constraint

$$\chi_{tot}(N, M) + 2\rho(N, M) = r(N - M) \tag{5.1}$$

where $\rho(N, M)$ is the number of contacts inside the free domain. Eq. 5.1 shows that $\chi_{tot}(N, M)$ must be even for r even. Specifically, for $r = 2$ adding a site to the contraction domain can change $\chi_{tot}(N, M)$ by only 0 or 2 units. Hence, the difference $\chi_{tot}(N, M) - 2\chi_1(N, M, j)$ in Eq. 3.13 must also be even for r even. The case $M = 0$ generates just the standard transition mode ΔG_m°. For $M = 1$ the transition modes are $\Delta G_m^\circ \pm 2J/(N - 1)$. For $M \geq 2$, and for any disposition of the contraction domain such that there are two adjacent constrained sites, it is always possible to increment $\chi_1(N, M, j)$ by 1 (up to the maximum) by constraining a site adjacent to one in state 0 to be itself in state 0. Therefore, for all $M \geq 2$, the difference $\chi_{tot}(N, M) - 2\chi_1(N, M, j)$ takes on all even integral values in the allowed ranges defined by Eqs. 3.16 and 3.18. Hence, for fixed M the subdistributions of transition modes for the Ising ring model are generated according to the following rule:

$$\Delta G_m(N, M, j) = \Delta G_m^\circ + 2j'(N - M)^{-1}J \tag{5.2}$$

where j' is not to be confused with j, the number of units frozen in state 1, but rather

$$j' = \begin{cases} \pm M & \text{for } M = 0, 1 \\ 0, \pm 1, \ldots, \pm M & \\ & \text{for } 0 \leq M \leq (N - 1)/2 \\ 0, \pm 1, \ldots, \pm (N - M) & \\ & \text{for } M \geq N/2 \end{cases} \tag{5.3}$$

Given the definition of $\Delta G_m(N, M, j)$ above and using arguments developed in section 4 for the fully connected Ising network, one may speculate that in the limit of large N each subdistribution for M fixed goes into a Gaussian with mean and variance

$$\mu(N, M) = \Delta G_m^\circ \tag{5.4a}$$

$$\sigma^2(N, M) = M(N - M)^{-2}J^2 \tag{5.4b}$$

However, a closer look at the values of the variance as a function of M, as shown in Fig. 5 for $N = 20$, indicates that a more accurate representation is given by the expression

$$\sigma^2(N, M) = \alpha M(N - M)^{-1}J^2$$
$$= \alpha(M/N + M^2/N^2 + \ldots)J^2 \tag{5.5}$$

where α is an *ad hoc* parameter independent of M. The form of Eq. 5.5 suggests that predicting the degeneracy of each mode for fixed M may be a quite difficult task for $r = 2$. The difference with the fully connected Ising network in the form of σ^2 draws attention to two points. First, the variance of the subdistribution depends on the value of N in the Ising ring,

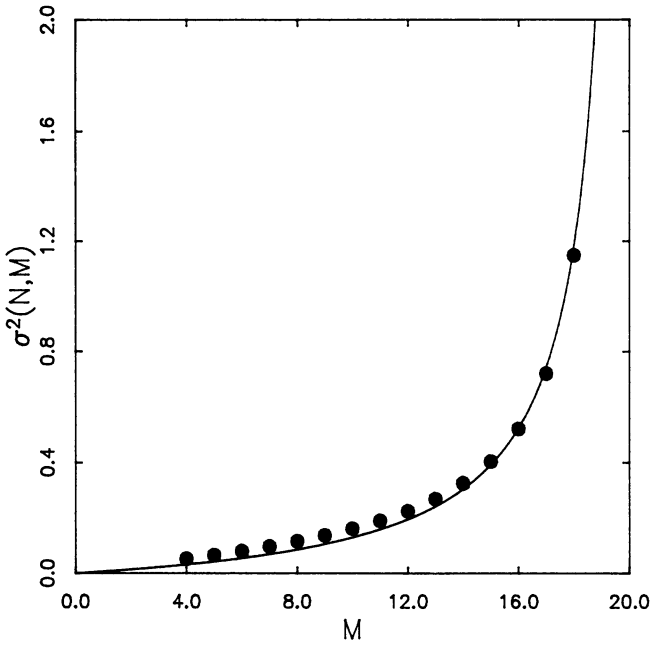

FIGURE 5 Dependence of the variance of the subdistributions of transition modes for fixed M as a function of M, in the case of the Ising ring network ($r = 2$) for $N = 20$ and $J = 1$. Each subdistribution is approximately a Gaussian, especially for values of $M > N/2$. The variance seems to grow according to the simple empirical expression $\sigma^2 = \alpha M/(N - M)$, depicted as a continuous line. The value of α is 0.131 ± 0.004.

while it is independent of N for the fully connected model. Second, the variance grows slowly with M in the Ising ring for most of the allowable values of M according to a polynomial in M/N, while it increases more rapidly with M in the fully connected model and in a linear fashion. As a consequence of this, in the limit of large N the subdistributions for fixed M are less spread out for $r = 2$ than $r = N - 1$. The values of transition modes tend to "diffuse" less around ΔG_m° as r decreases. This difference reveals the contribution of intermediate configurations to the overall behavior of the system.

The overall distribution of transition modes can be seen as the superposition of Gaussian terms, with mean and variance given by Eqs. 5.4a and 5.5, each term being weighted by the binomial $C_{N,M}$. At present we do not have an analytical expression for the overall distribution, owing to the difficulty of integrating over M terms containing Eq. 5.5 in exponential form. Fig. 6 shows the computer-generated distribution for $N = 20$. The expected symmetry about ΔG_m° is evident, and it can be confirmed that the modes occur at the values specified by Eq. 5.2. A remarkable feature is that the distribution is sharply peaked around the standard transition mode, which can be understood quite well in terms of the decreased tendency of the modes to diffuse around this value. Additional complications in computing the overall distribution arise from the fact that for finite N the transition modes are not uniformly distributed in the range dictated by Eq. 3.19, which makes it quite difficult to assess the degeneracy in an analytical way. The problem is to determine the number of distinct transition modes for a given number of units, N. It is clear from Eq. 5.2 that several different values of M and j' may generate the same mode value. The problem of assessing how many distinct transition modes are allowed in the Ising ring for a given value of N is completely analogous to the problem of finding the number of distinct values of the ratio

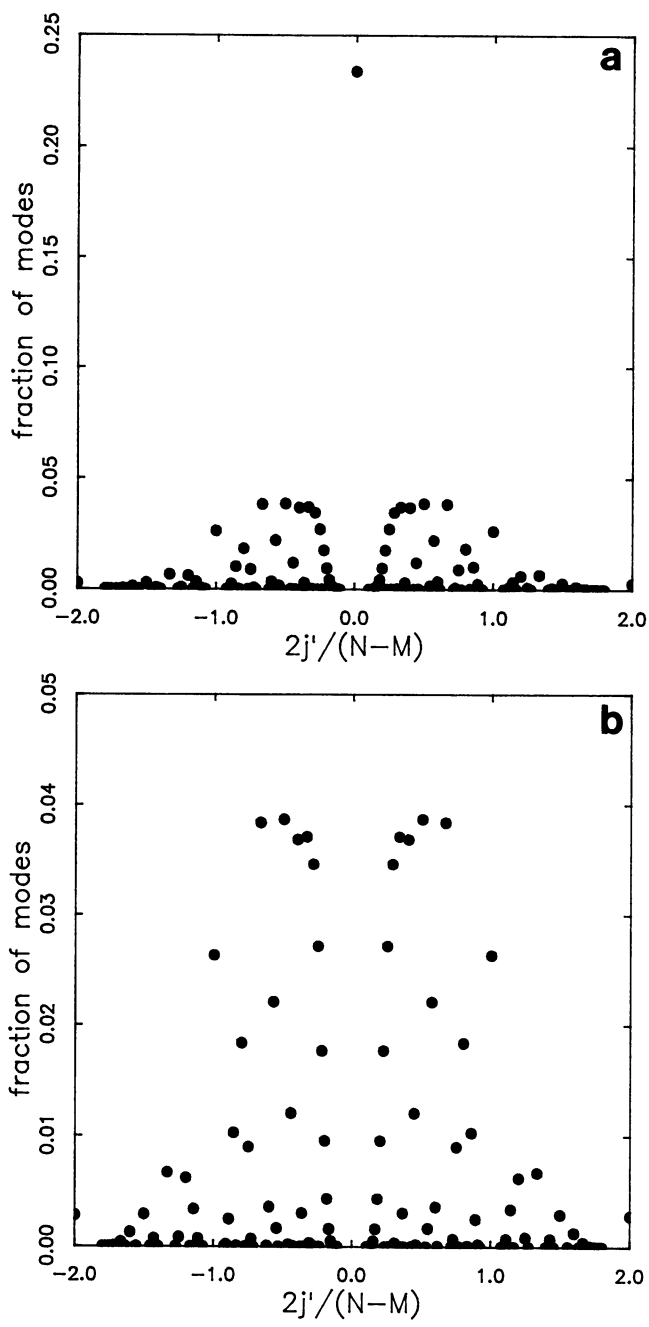

FIGURE 6 (*a*) Distribution of transition modes for the Ising ring network ($r = 2$) for $N = 20$. The degeneracy of each mode has been normalized by $\nu_N = 3^N - 2^N$ to yield the probability of occurrence (or fraction of modes) shown. The values are plotted versus $2j'/(N - M)$ according to the definition given in Eq. 5.2, with values of $\Delta G_m^\circ = 0$ and $J = 1$ used for the sake of simplicity. Notice how the standard transition mode stands out relative to all other modes. (*b*) Details of the distribution shown in (*a*) that emphasize the complexity of the landscape of transition modes.

$j'/(N - M)$, given the rules in Eq. 5.3 and $M = 0, 1 \ldots, N - 1$. This problem, which may sound like a trivial task, is instead a rather fundamental problem in analytical number theory, and its exact solution is unknown. The distinct rational numbers $j'/(N - M)$ form so-called Farey sequences (25), and the number of distinct transition modes for the Ising ring is given by

$$\zeta_N = 1 + \Phi(N) \tag{5.6}$$

where $\Phi(N)$ is the number of rational numbers m/n such that $1 \leq m, n \leq N$. A result of analytical number theory (25) is that this arithmetic function satisfies

$$\Phi(N) = 3N^2/\pi^2 + 0(N \ln N) \tag{5.7}$$

Hence,

$$\zeta_N \approx 3N^2/\pi^2 \tag{5.8}$$

and the number of distinct transition modes grows as N^2, a result that should be compared with ν_N, which grows as 3^N. Since the number of distinct modes for $r = N - 1$ is clearly $\zeta_N = 2N - 1$, it is appropriate to analyze the dependence of ζ_N on r. The results are shown in Fig. 7 *a* for different values of N. The number of distinct modes first increases and then decreases sharply when r approaches its maximum value $r_{max} = N - 1$. The results shown in Fig. 7 *a* suggest that proper rescaling of the variables should yield a "universal" function. Indeed, a replot of ζ_N divided by N^3 versus the logarithm of $1 - r/r_{max}$ indicates the existence of a "law of corresponding states" that connects ζ_N to the ratio r/r_{max}. The validity of such a seemingly universal relationship demands an analysis of large values of N. However, one should consider the computational complexity of the problem, of the order 3^N, since all transition modes must be exhausted iteratively. The algorithm takes three times longer whenever N is increased by only one unit. On our HP Apollo 9000/730 work station, running at 76 MIPS and 27 MFLOPS, the case $N = 20$ is exhausted in about 1 day. A Cray supercomputer would not do much better than that, but a teraflop, massive parallel supercomputer would handle the case $N = 40$ in a reasonable time frame. In addition to supercomputing capabilities one clearly needs to investigate the nature of the relationship between ζ_N and r in mathematical terms, perhaps trying to generalize the fundamental result of analytical number theory (25) that applies to the case $r = 2$ (see Eq. 5.8). The results shown in Fig. 7 *b* will be extremely helpful in analytical terms in the future investigation of this problem.

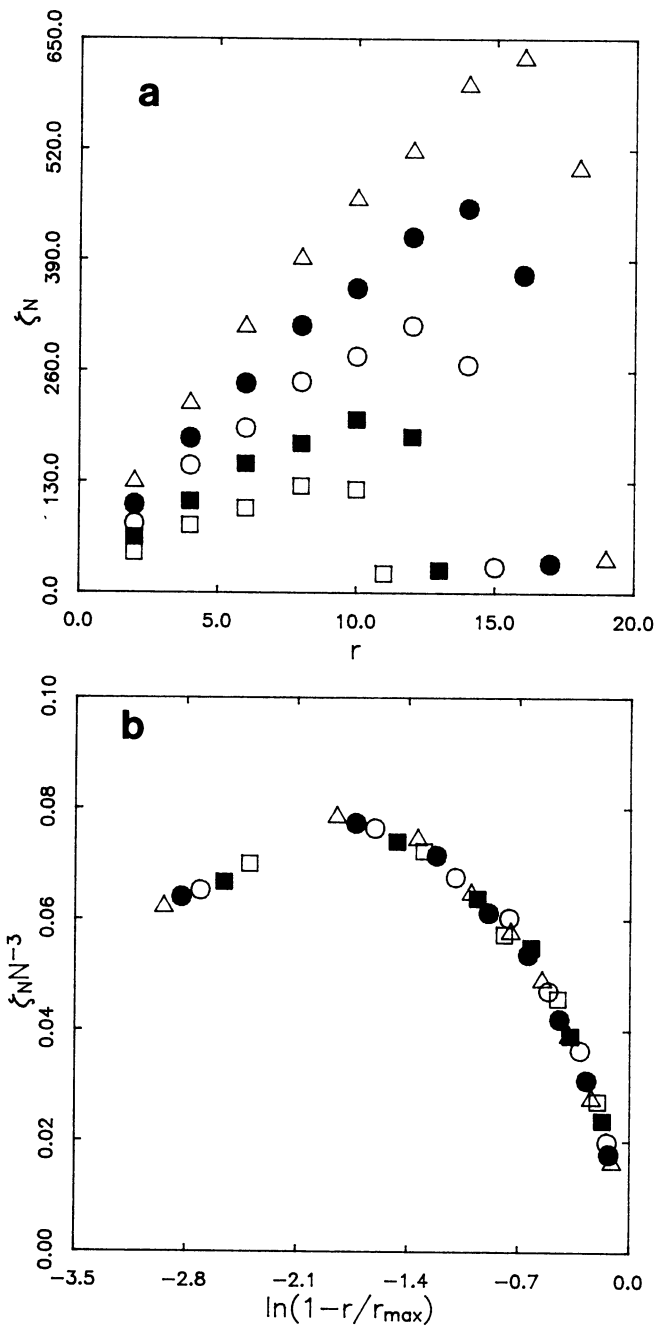

FIGURE 7 (*a*) Dependence of ζ_N on r, for different values of N as follows: (□) 12; (■) 14; (○) 16; (●) 18; ( ) 20. (*b*) Replot of the data shown in (*a*), with $r_{max} = N - 1$. Symbols refer to different values of N, as in (*a*).

6. CONNECTION WITH MEAN-FIELD TREATMENTS

The concept of transition mode has some quite interesting applications. The first example is provided by the connection with the mean-field treatment of cooperative transitions. In the limit of large N the ratio j/N can be seen to approximate the probability, θ, of finding a unit in state 1. The average free energy for the $0 \rightarrow 1$ transition computed in terms of statistical thermodynamics is evidently

$$\Delta G_{0\rightarrow 1} = -k_B T \ln\{\theta/(1 - \theta)\} \tag{6.1}$$

This free energy is a measure of the work spent by the system in switching one unit from state 0 to state 1 when the probability of finding state 1 is θ. The transition mode obtained by constraining $M = N - 1$ units for $j = N\theta$ is a good approximation of $\Delta G_{0\rightarrow 1}$, since it gives the amount of work needed to increase the number of units in state 1 from j to $j + 1$, given a particular value of j. We take the fully connected Ising network as a model for the transition modes and

apply Eq. 4.2 with $M = N - 1$ to obtain an expression for $\Delta G_{0\rightarrow 1}$ as follows:

$$\Delta G_{0\rightarrow 1} = \Delta G_m(N, N-1, j)$$
$$= \Delta G_m^\circ + (N - 1 - 2j)J \quad (6.2)$$

In the limit of large N one has

$$-k_B T \ln\{\theta/(1-\theta)\} = \Delta G_m^\circ + N(1-2\theta)J$$
$$= \Delta G_m^\circ + (1-2\theta)J' \quad (6.3)$$

which is the familiar form for the function θ in the mean-field approximation (1, 9). Notice how this result is derived in a rather straightforward way from consideration of the transition modes of an Ising network. The main features of the mean-field approach can be given a precise interpretation in terms of the parameters of the Ising network. For example, the mean free energy of the 0→1 transition is the value of $\Delta G_{0\rightarrow 1}$ at $\theta = 1/2$ (1, 11). This is just the value of the standard transition mode ΔG_m°. The critical parameter of the mean-field approximation defining the divergence of the derivative of θ is obtained by equating the first derivatives of the two sides of Eq. 6.3 for $\theta = 1/2$, so that

$$J_c' = 2k_B T \quad (6.4)$$

The critical value of the interaction energy is positive, as expected for cooperative transitions that destabilize the intermediates, and is just twice the value of $k_B T/N$.

7. ANALYSIS OF THE PARTITION FUNCTION

The partition function of an Ising network can be constructed in a rather straightforward way from the distribution of transition modes. The recipe taken from statistical mechanics (1) gives

$$Z = \sum_{i=0}^{N} \mathscr{P}_i(\omega)\lambda^i \quad (7.1)$$

Here $\mathscr{P}_i(\omega)$ is a polynomial in the interaction constant ω as defined in Eq. 3.3, λ is an ad hoc variable including the equilibrium constant K in Eq. 3.2, and i is the number of units in state 1. When the 0→1 transition is driven by the temperature of the heat bath the variable λ is simply equal to K, and Z is the partition function of a canonical ensemble. When the 0→1 transition is driven by the binding of a ligand at constant temperature, the variable λ is the product Kx, where x is the ligand activity, and Z is the partition function of a grand canonical ensemble. In either case the partition function is the sum of 2^N site-specific terms, the weights of which are computed relative to the reference configuration where all units are in state 0 (9). This makes the calculation of each term quite simple from consideration of transition modes. Any configuration can be generated from the reference configuration by freezing M units in state 0 and allowing the remaining $N - M$ units in the free domain to switch to state 1. The free energy change associated with this transition is evidently

$$\Delta G(N, M) = (N - M)\Delta G_m(N, M, 0) \quad (7.2)$$

and scales with the transition mode associated with it according to the number of units in the free domain. Hence, the coefficients of the partition function are derived from a subset of the transition modes by letting $j = 0$. Using the definition of transition mode in Eq. 3.6 it is easy to see that $\chi_0(N, M, 0) = 0$ and therefore

$$\Delta G(N, M) = (N - M)\epsilon + \chi_1(N, M, 0)J \quad (7.3)$$

where $\chi_1(N, M, 0)$ is the number of 01 pairs across the boundary between the free and contraction domains when M units in the contracted domain are in state 0 and $N - M$ units in the free domain are in state 1. The associated coefficient is of the form

$$A(N, i) = \exp(-\Delta G(N, N-i)/k_B T) = \omega^m K^i \quad (7.4)$$

where i denotes the number of units in state 1 and m is the value of $\chi_1(N, N - i, 0)$ and is of course a function of i. The partition function 7.1 is the sum of all A's over i and all possible values of m for a given value of i. The variable λ replaces K in Eq. 7.1 and is independent of m. The possible values of m for a given value of i define the polynomial

$$\mathscr{P}_i(\omega) = \sum g_{m,i}\omega^m \quad (7.5)$$

where the sum extends to all possible values of m and $g_{m,i}$ is the degeneracy, or microcanonical component, associated with ω^m.

Some of the topological properties of the partition function of Ising networks can be explored by studying the effect of the dimensional embedding on lattices with the same connectivity r. Once r is fixed, the spectrum of m values for a given value of i in the polynomial 7.5 can be computed for a one-dimensional and a two-dimensional Ising network. The results of these calculations are shown in Fig. 8 for $N = 16$ and $r = 4$. The two-dimensional network is a torus formed by a ring of four 4-unit rings, with each unit connected to two units in the same ring and two other units in the adjacent rings. The one-dimensional version of this network is shown in Fig. 9. Since there is substantial overlap in the spectra obtained in the two cases, the properties of one-dimensional Ising networks may be quite useful in the analysis of Ising networks in higher dimensions with equivalent connectivity. Consideration of the transition modes associated with networks in different dimensions should open an intriguing new way of approaching the Ising problem.

8. A SIMPLE MODEL FOR MACROMOLECULAR RECOGNITION

The results outlined in the foregoing analysis may be used to develop an approximate theory for macromolecular recognition. A fundamental problem in physical biochemistry and computational chemistry is to predict the free energy of

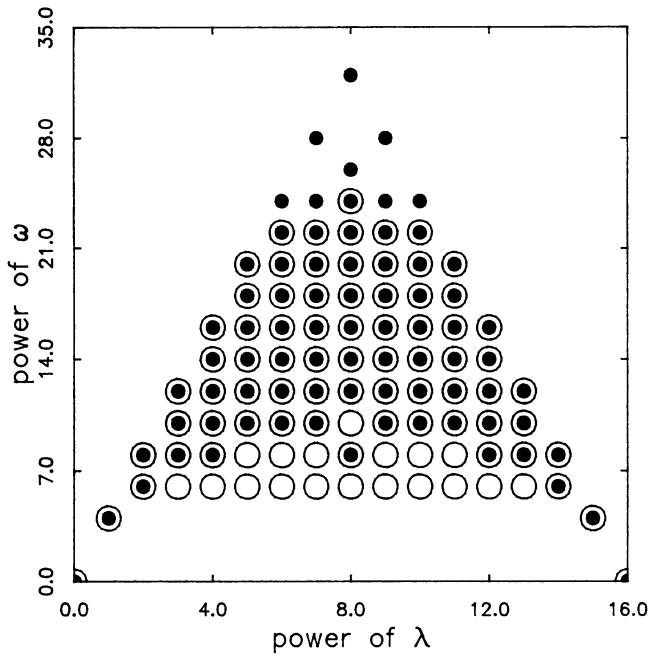

FIGURE 8 Spectrum of m values, or powers of ω in Eq. 7.5, as a function of the number of units in state 1, which is the same as the power of λ in the partition function 7.1. The values depict the results obtained for a one-dimensional (○) and a two-dimensional (●) Ising network with $N = 16$ and $r = 4$. Over three-fourths of the total values are the same for the two networks. The well-defined upward shift of the values for the two-dimensional network indicates a higher cooperativity compared to the one-dimensional case and reveals the effect of lattice dimensionality.

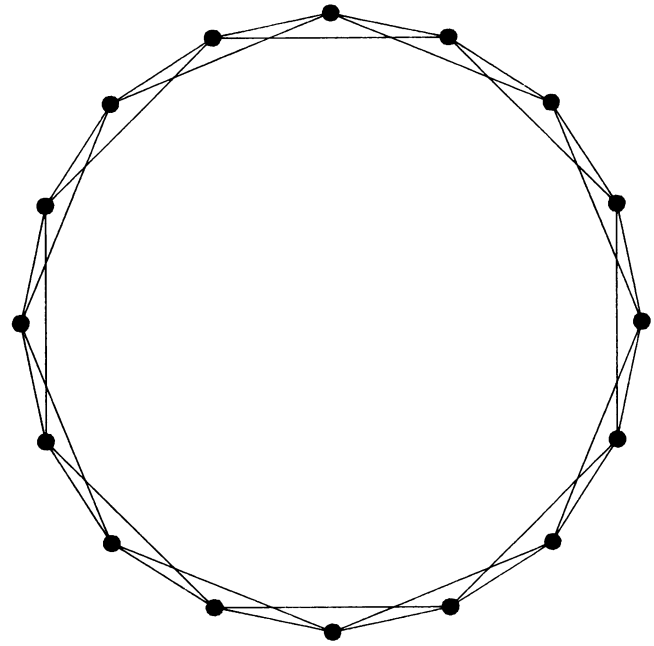

FIGURE 9 One-dimensional Ising network with $N = 16$ and $r = 4$. Each unit contacts four other adjacent units in a way that minimizes the distance. This network is the one-dimensional version of a two-dimensional torus with $N = 16$ and the same value of r.

interaction from a knowledge of structural components. The approaches being used entail electrostatic and molecular dynamics calculations (26–28) and take into account the detailed functional groups involved in the interaction of a biological macromolecule with a ligand. Here we seek to develop a simplified treatment of this problem that is somewhat phenomenological. The goal is to formulate a suitable model that is able to capture the essential features of macromolecular recognition and could serve as a starting point for the development of more detailed schemes.

Let us consider two surfaces, A and B, with A containing N acceptor subsites for N donor subsites of B. Surface A is assumed to be totally inert, i.e., its energetic state is the same when free or bound to B. The donors of B can exist in two energetically equivalent states, 0 and 1. When surface B is free, all donors are in state 0. When surface B is bound to surface A all donors switch to state 1 in an induced-fit fashion. Each pair "donor in state 1:acceptor" provides a free energy of stabilization, $\Delta G°$, across the A–B interface of the bound complex. State 0 can be interpreted as a neutral state with the pair "donor in state 0:acceptor" providing a zero free energy of stabilization to the bound complex. Hence, the free energy of binding of surface B to A is simply $\Delta G_0 = N\Delta G°$. Note that this conceptual framework can also be used in the analysis of the protein folding problem by allowing the two surfaces A and B to be distinct domains of the same macromolecule. In this scenario protein folding becomes a problem of macromolecular self-recognition. Assume now that a number of site-specific "mutations" are made on surface B. We assume that any mutation may have the effect of freezing one or more donors in a particular state 0 or 1, because these are the only stable states accessible to any given subsite. In principle, there is no way one can predict the effect of the mutation on the value of ΔG for binding B to A, because the mutation can act locally at the subsite where it applies or propagate to distant sites. However, regardless of the extent and precise architecture of the perturbation, we know that the surface B free will assume only one of the 2^N possible configurations allowed for the manifold of donors. In other words, surface B can only assume a configuration that belongs to the ensemble of configurations consistent with the intrinsic properties of each donor, independent of the nature of the mutation applied to it. Assume now that the mutation has frozen M donors, j of which are in state 1, and that the probabilities of freezing a donor in state 0 or 1 are the same. In mathematical terms the effect of the mutation is that of generating a contraction domain in the system. The free energy of binding of this mutant to surface A can be computed as follows. A total of $N - M$ donors are free to switch to state 1 when bound to surface A. These donors provide a free energy change $(N - M)\Delta G°$. Among the frozen donors, $M - j$ remain in state 0 even when bound to surface A. These donors provide no contribution to the binding free energy. On the other hand, the j donors frozen in state 1 provide an additional term $j\Delta G°$ to the total free energy of binding,

which is then

$$\Delta G(N, M, j) = (N - M + j)\Delta G^{\circ} \quad (8.1)$$

The binding free energy difference between the mutant and the wild-type surface B is

$$\Delta\Delta G(N, M, j) = -(M - j)\Delta G^{\circ} \quad (8.2)$$

In this simple model any mutation is expected to reduce the binding affinity, unless the number of donors frozen in state 1 coincides with the total number of frozen donors M. By changing M and j the entire spectrum of possible $\Delta\Delta G$ values can be generated. This is the ensemble of free energy perturbations that is to be expected in the system under consideration. However, not all $\Delta G(N, M, j)$ values are equally likely to occur, due to the intrinsic differences in the weighting of the various configurations. For a fixed value of M the values of $\Delta G(N, M, j)$ are distributed as a Gaussian with mean and variance

$$\mu(N, M) = (N - M/2)\Delta G^{\circ} \quad (8.3a)$$

$$\sigma^2(N, M) = (M/4)\Delta G^{\circ 2} \quad (8.3b)$$

Hence, the overall distribution of $\Delta G(N, M, j)$ values that can be accessed experimentally can be written in the form

$$P(x) = \sum_{M=0}^{N-1} w(N, M)\{2\pi\sigma^2(N, M)\}^{-1/2} \exp\{-[x - \mu(N, M)]^2/2\sigma^2(N, M)\} \quad (8.4)$$

where x is the desired value of $\Delta G(N, M, j)$ and $w(N, M)$ is a weighting factor given by

$$w(N, M) = 2^M C_{N,M}/\nu_N \quad (8.5)$$

This model provides a simple conceptual framework for understanding macromolecular recognition. The assumption of the existence of a unique "energy space" defined by the alternative states allowed for each individual donor makes it possible to analyze mutations of different natures, either single- or multi-site, using essentially the same formalism. Multiple mutations, in fact, act on the system in the same way as single mutations by generating contraction domains of various sizes and distributions of frozen donor subsites in state 0 or 1. The predictions of this model can be tested in a straightforward way by analyzing free energy profiles obtained for macromolecular systems and their mutant derivatives. In so doing, one should realize that the form of the weighting factor $w(N, M)$ in Eq. 8.5 can be made arbitrary, since this quantity is clearly independent of x. The predictive value of the model, and hence its relevance in practical applications, stems from the Gaussian form of each subdistribution, the mean and variance of which are defined a priori. In practice, one could assume that the landscape of $w(N, M)$ values might be quite different from the one predicted by Eq. 8.5 for a number of reasons. For example, the finite sample of free energy values obtained experimentally may arbitrarily bias the weight of particular subdistributions of $\Delta G(N, M, j)$ values for certain values of M. Certain contraction patterns associated with particular values of M may become predominant in the overall distribution if mutations concentrate on a limited structural area of interest. More importantly, one may think of the surface-surface recognition as introducing a "filter" in the ensemble of subdistributions. This filter acts "externally" only on the values of $w(N, M)$ and does not alter the Gaussian nature of each subdistribution, which reflects the "internal" properties of surface B. Therefore it seems appropriate to cast Eq. 8.4 in a very general form as follows:

$$P(x) = \sum_{M=0}^{N-1} w(N, M) \exp\left\{ -\frac{[x - \mu(N, M)]^2}{2\sigma^2(N, M)} \right\} \quad (8.6)$$

by interpreting the weighting factors $w(N, M)$ as generalized filters of the ensemble of subdistributions. Notice that the term $\{2\pi\sigma^2(N, M)\}^{-1/2}$ can be incorporated into the $w(N, M)$ filter without loss of generality, since it does not depend on x.

The relevant parameters of the model can be obtained from an analysis of experimental data in the following way. The overall distribution $P(x)$ is clearly a combination of Gaussian terms, regardless of the particular form of the factors $w(N, M)$ in Eq. 8.6. Hence, the distribution of $\Delta G(N, M, j)$ values obtained experimentally should be analyzed in terms of a combination of Gaussian terms, the mean and variance of which are to be considered as independent parameters. Each Gaussian term should be weighted properly using another set of independent parameters for the filters $w(N, M)$. Once the best-fit values of μ and σ^2 are determined for all Gaussian terms, a plot of σ^2 versus μ should be constructed. The model predicts that such a plot would be a straight line. In fact, on eliminating M from Eq. 8.3 one has

$$\sigma^2 = \Delta G^{\circ}(\Delta G_0 - \mu)/2 \quad (8.7)$$

The intercept in this plot gives ΔG_0, the free energy of binding of the unperturbed system where all donor subsites are free, while the slope gives half the value of the free energy of binding provided by a single donor in state 1:acceptor pair across the A–B interface. Hence, the ratio $\Delta G_0/\Delta G^{\circ}$ gives N, the number of subsites in the system.

We are now in the position of generalizing the foregoing analysis to the more relevant and interesting case where interactions exist among the donor subsites of surface B. We use a mean-field type of interaction by assuming that each donor is in contact with $r = N - 1$ other donors. Two donors in contact interact according to an energy J only if they are in different states. Here we employ the same rules as those outlined in section 3. The architecture of this fully connected Ising network is such that the state of any given donor in the surface will be "felt" by all others, as in the case of a true field. The effect of a mutation on surface B is more complex than that seen in the case of independent subsites. When M units are frozen, j of which in state 1, the energetic state of the surface can be predicted from the number of donors in

states 0 and 1 and the interactions among them as follows

$$E_B(\text{free}) = j(N - j)J \tag{8.8}$$

When the surface is bound all donors in the free domain switch to state 1, while the donors in the contrated domain remain frozen. The new energetic state of the surface is

$$E_B(\text{bound}) = (N - M + j)(M - j)J \tag{8.9}$$

In the case of surface A we retain the assumption that it is inert and its energetic state is not affected by ligation. The energetic state of the interface between A and B is computed by counting the number of "donor in state 1:acceptor" pairs. The free energy of binding of the two surfaces is evidently

$$\Delta G(N, M, j) = (N - M + j)\Delta G^\circ + (N - M)(M - 2j)J \tag{8.10}$$

One sees quite clearly that the free energy of binding is closely related to the transition mode of surface B. Hence, the properties of the distribution of $\Delta G(N, M, j)$ values may be expected to have a bearing on those dealt with in section 4. Indeed, for fixed M, $\Delta G(N, M, j)$ is symmetric around $\Delta G(N, M,M/2)$ and the $\Delta G(N, M, j)$ values are uniformly distributed with a spacing of $\Delta G^\circ - 2(N - M)J$. The subdistribution for M fixed is a Gaussian with mean and variance

$$\mu(N, M) = (N - M/2)\Delta G^\circ \tag{8.11a}$$

$$\sigma^2(N, M) = (M/4)\{\Delta G^\circ - 2(N - M)J\}^2 \tag{8.11b}$$

Again, the overall distribution of $\Delta G(N, M, j)$ can be written as the superposition

$$P(x) = \sum_{M=0}^{N-1} w(N, M) \exp\left\{ - \frac{[x - \mu(N, M)]^2}{2\sigma^2(N, M)} \right\} \tag{8.12}$$

where x is the desired value of $\Delta G(N, M, j)$ and $w(N, M)$ is the generalized filter for the value of M. This model of interacting donor subsites on surface B predicts that σ^2 would depend on μ as follows:

$$\sigma^2 = \frac{(\Delta G_{opt} - \mu)\{\Delta G^{\circ 2} + 2J\Delta G_{opt} - 4J\mu\}^2}{2\Delta G^{\circ 3}} \tag{8.13}$$

where $\Delta G_{opt} = N\Delta G^\circ$ is the optimized value of the free energy of binding, obtained when all donors are in state 1 in the bound form of surface B. The variance σ^2 is a cubic function of the mean μ. We recall that in the case of independent donor subsites, which is obtained from Eq. 8.13 for $J = 0$, a linear dependence of σ^2 on μ is expected. Hence, an important property of the system, i.e., whether individual subsites involved in the recognition process are coupled together in a cooperative fashion, can be extracted from an analysis of experimental data using the predictions of our model.

The distribution for the free energy of binding of thrombin-hirudin interaction is shown in Fig. 10. A total of 67 mutants of hirudin have been studied under identical solution conditions (29, 30), and the resulting values of the standard free energy of binding have been grouped in separate intervals if found to be within ± 0.2 kcal/mol from preassigned values along the x-axis. We notice that the landscape of $\Delta\Delta G$ values spans a range of nearly 10 kcal/mol and is distinctly multimodal. The free energy of binding of the wild-type hirudin is −17.93 ± 0.09 kcal/mol (31), which makes thrombin-hirudin interaction one of the most specific protein-protein interactions known in biology. The interval of ±0.2 kcal/mol used in grouping the free energy values is the typical upper bound for experimental error in these measurements (31, 32). Hence, any two $\Delta\Delta G$ values in Fig. 10 differ by at least 0.4 kcal/mol and are significantly different in statistical terms. The hirudin molecules studied are single- and multi-site mutants, and the mutations involve polar and apolar side chains to test the contribution of specific electrostatic and hydrophobic interactions to the stability of the thrombin-hirudin complex. Furthermore, the mutations involve the entire surface of recognition, as revealed by X-ray crystallography (33), and not just localized areas.

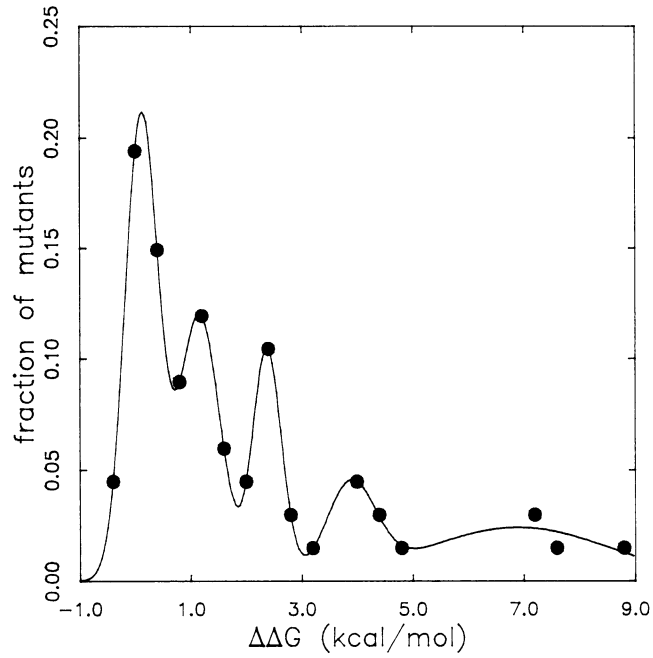

FIGURE 10 Distribution of binding free energies for thrombin-hirudin interaction. The ΔG values obtained for a total of 67 hirudin mutants have been grouped in intervals of 0.4 kcal/mol and expressed as $\Delta\Delta G$ = ΔG(mutant) − ΔG (wild type), with ΔG (wild type) = −17.93 ± 0.09 kcal/mol. The ordinate value represents the fraction of mutants for each free energy interval. The continuous line is the best fit obtained according to Eq. 8.12 using the superposition of five Gaussian terms. The best-fit values of the mean and variance of each Gaussian are shown in Fig. 11. The best-fit values of the generalized filters are shown in Fig. 12.

Both the size of the statistical sample and the nature and distribution of the mutations indicate that the data shown in Fig. 10 should provide an unbiased and most relevant case to test the prediction of our approximate treatment. Here we model hirudin as surface B and thrombin as surface A. The continuous line depicts the best fit of the experimental data

to a superposition of Gaussian terms, the mean and variance of which is given in Fig. 11. The variance first increases for values of μ close to the ΔG of the wild type and then decreases around $\mu = -16$ kcal/mol and eventually increases dramatically for $\mu = -11$ kcal/mol. Quite clearly, the points in Fig. 11 do not follow a straight line. Application of Eq. 8.13, on the other hand, gives an excellent representation of the data, thereby indicating that the recognition subsites of the hirudin molecule are coupled in a cooperative fashion. The number of such subsites predicted by the model is $N = 12 \pm 3$, each providing -1.5 ± 0.3 kcal/mol to the free energy of stabilization across the thrombin-hirudin interface. The number of ion pairs and hydrogen bonds across this interface is 8 and 13, respectively (33). Considering the approximations of our model, a result of $N = 12 \pm 3$ is quite reasonable. The interaction energy is estimated from analysis of the data in Fig. 11 to be $J = -0.10 \pm 0.04$ kcal/mol. This value indicates the cost per contact of switching one donor of the contraction domain to state 1. For example, if a mutation causes $M = 1$ and $j = 1$, then the loss in free energy of binding is $-(N - 1)J = 1.1$ kcal/mol. Also, the value of J ($J < 0$) indicates that subsite pairs in different states are stabilized with respect to pairs in the same state, as seen in the case of negatively cooperative systems (3). The value of $\Delta G_{opt} = N\Delta G°$ is about -18 kcal/mol, which is practically identical to the free energy of binding of the wild-type hirudin. This suggests that hirudin binding to thrombin has little room left for optimization—a conclusion that can hardly be disputed, given the specificity of the interaction—and that practically all recognition subsites in the wild type are in state 0 when free and state 1 when bound. A final comment should be made on the form of the generalized filter terms $w(N, M)$. The values of M for each Gaussian subdistribution in Fig. 12 can be reconstructed from the values of μ, N, and $\Delta G°$, using Eq. 8.11a, and used to construct a plot of the values of w, as determined experimentally, versus M. Such a plot is given in Fig. 12 and shows that w decreases monotonically with M according to a simple exponential law.

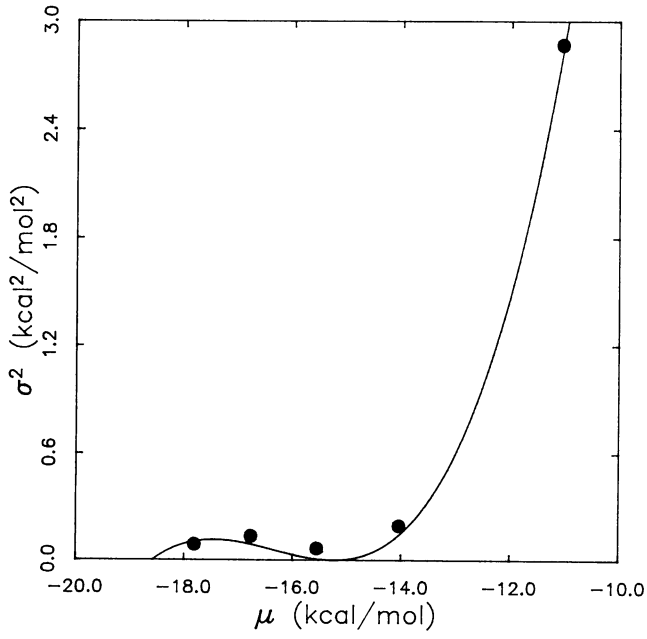

FIGURE 11 Values of the mean and variance of each Gaussian term involved in Eq. 8.12, as determined from analysis of the experimental data shown in Fig. 10. The continuous line is the best fit obtained according to Eq. 8.13 using the parameter values: $\Delta G° = -1.5 \pm 0.3$ kcal/mol, $J = -0.10 \pm 0.04$ kcal/mol, $N = 12 \pm 3$.

9. DISCUSSION

The concept of transition mode introduced here arises from consideration of the site-specific properties of lattice models and emphasizes the role played by intermediate states in shaping the energetics of the system as a whole. The landscape of free energy values for the elementary transition $0 \rightarrow 1$ in a system of interacting units encapsulates all the important thermodynamic properties of the network. In particular, the free energy terms entering the definition of the partition function of the system are derived from the modes by simple transformations. It is to be hoped that further investigation

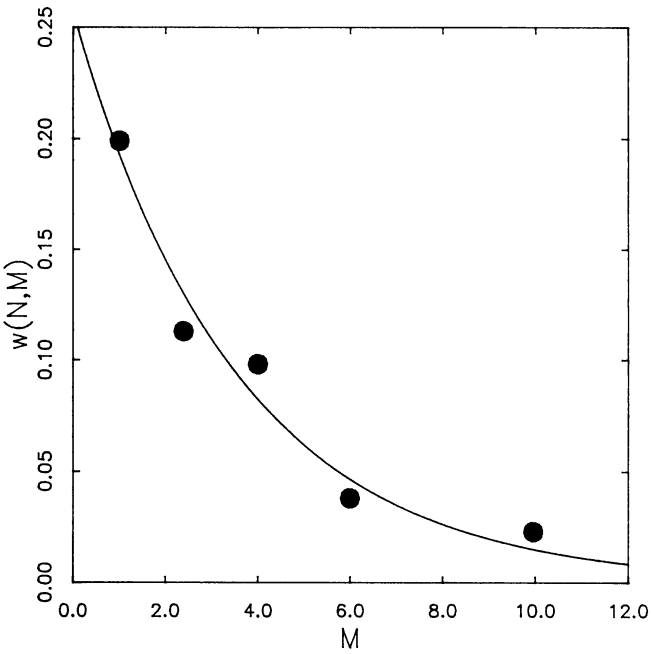

FIGURE 12 Values of the generalized filter of each Gaussian term involved in Eq. 8.12, as determined from analysis of the experimental data shown in Fig. 10, plotted versus M. The values of M were calculated from the values of μ in Fig. 11, using the best-fit values of N and $\Delta G°_m$. The continuous line is the best fit obtained according to the empirical expression $w(N, M) = \alpha \exp(-M/\beta)$, with $\alpha = 0.26 \pm 0.03$ and $\beta = 3.5 \pm 0.5$. The exponential nature of the dependence of $w(N, M)$ on M suggests that the probability of freezing M sites resembles a Poisson process. The value of α represents the probability that a mutation produces no effect in the ensemble of hirudin subsites. The value of β is the "relaxation" value of M or the size of the contraction domain that reduces the probability α by a factor e. The "continuous" nature of the exponential relationship between $w(N, M)$ and M, interesting as it may be, has a solely empirical value and should not induce one to overlook the fundamental nature of the filter values as "discrete" quantities.

of the components determining the form of the subdistributions for given values of M for networks in two or higher dimensions will reveal some useful patterns that can be exploited in the formulation of the partition function of the system. We have seen that the architecture of the interaction network and its dimensionality uniquely determine the shape of the distribution of transition modes, but at the same time, remarkable similarities exists among networks in different dimensions that share the same value of r. Specifically, most of the transition modes and free energy terms of the partition function for two-dimensional Ising networks are contained in the distribution of modes for one-dimensional Ising networks with the same value of r. Hence, one can expect the partition function of a two-dimensional Ising network with $r = 4$ to have a bearing on that of a one-dimensional Ising network with $r = 4$. The connection between solutions of the Ising problem in one and two dimensions is likely to be stronger than imagined so far. Onsager's landmark work on the two-dimensional Ising problem (34) and the general theorem of Lee and Yang on the zeros of the partition function (35, 36) make it possible to explore the nature of this connection in an analytical way.

In addition to the significant role that the concept of transition mode can play in the analysis of basic properties of lattice statistics, including a transparent interpretation of classical mean-field approaches as shown in section 6, transition mode distributions have proved helpful in the analysis of the problem of macromolecular recognition. It is quite appropriate to think of this phenomenon as a cooperative process that involves a number of individual components coupled together. A crude approximation of the way macromolecular surfaces may recognize each other through an interface involving many recognition subsites emphasizes the role of transition modes in setting the rules for the overall energetics. Our treatment has yielded a satisfactory representation of the distribution of binding free energies for the biologically relevant interaction of thrombin with hirudin. Analysis of this distribution has provided some useful information on basic aspects of the interaction, such as the number of recognition subsites involved and the energy balance for binding and cooperative coupling among the them. Due to the widespread use of recombinant DNA technology as a tool for dissecting structure-function relationships in macromolecular systems, similar distributions can be constructed for other protein-ligand, protein-protein, or protein-DNA interactions. The approximate treatment presented here provides a simple phenomenological model to extract useful information on the system from an analysis of mutants. Further investigation of the properties of transition mode distributions for networks with arbitrary interactions and components will make it possible to refine our approach to macromolecular recognition by incorporating structurally relevant details.

In this paper we have explicitly avoided the analysis of statistical networks composed of nonequivalent units, such as linear or branched chains of interacting units (3), heterogeneous lattices (11), or networks that can undergo global allosteric transitions (3). A detailed analysis of these networks goes beyond the scope of the present work and will be reported elsewhere.

We are grateful to Dr. Stuart Stone (MRC, Cambridge, England) for providing his results on the free energies of thrombin-hirudin interaction prior to publication.

This work was supported by National Science Foundation grant DMB91-04963 and a grant from the Lucille P. Markey Charitable Trust. E. Di Cera is an Established Investigator of the American Heart Association.

REFERENCES

1. Hill, T. L. 1960. Statistical Mechanics. Dover, New York.
2. Creighton, T. E. 1992. Protein Folding. Freeman, New York.
3. Hill, T. L. 1984. Cooperativity Theory in Biochemistry. Springer, Berlin.
4. Stanley, H. E. 1976. Introduction to Phase Transitions and Critical Phenomena. Oxford University Press, New York.
5. Freire, E., and K. P. Murphy. 1991. Molecular basis of cooperativity in protein folding. *J. Mol. Biol.* 222:687–698.
6. Ackers, G. K., M. L. Doyle, D. W. Myers, and M. A. Daugherty. 1992. Molecular code for cooperativity in hemoglobin. *Science (Washington DC).* 255:54–63.
7. Domb, C., and M. S. Green. 1972. Phase Transitions and Critical Phenomena. Academic, New York.
8. Itzykson, C., and J-M. Drouffe. 1989. Statistical Field Theory. Cambridge University Press, Cambridge, England.
9. Di Cera, E. 1990. Thermodynamics of local linkage effects: contracted partition functions and the analysis of site-specific energetics. *Biophys. Chem.* 37:147–164.
10. Beroza, P., D. R. Fredkin, M. Y. Okamura, and G. Feher. 1991. Protonation of interacting residues in a protein by a Monte Carlo method: application to lysozyme and the photosynthetic reaction center of *Rhodobacter sphaeroides*. *Proc. Natl. Acad. Sci. USA.* 88:5804–5808.
11. Di Cera, E. 1992. Mean-field treatment of local binding processes. *J. Chem. Phys.* 96:6515–6522.
12. Glauber, R. J. 1963. Time-dependent statistics of the Ising model. *J. Math. Phys.* 4:294–307.
13. Poland, D., and H. A. Scheraga. 1970. Theory of Helix-Coil Transitions in Biopolymers. Academic Press, New York.
14. Simha, R., and R. H. Lacombe. 1971. One-dimensional cooperative kinetic model. Equilibrium solution for finite chains. *J. Chem. Phys.* 55:2936–2939.
15. Lewis, P. N., N. Gō, M. Gō, D. Kotelchuck, and H. A. Scheraga. 1970. Helix probability profiles of denatured proteins and their correlation with native structures. *Proc. Natl. Acad. Sci. USA.* 65:810–815.
16. Di Cera, E., and Z-Q. Chen. 1993. The binding capacity is a probability density function. *Biophys. J.*, 65:164–170.
17. Holland, J. H. 1975. Adaptation in Neural and Artificial Systems. The University of Michigan Press, Ann Arbor, MI.
18. Eigen, M., J. McCaskill, and P. Schuster. 1988. Molecular quasi-species. *J. Phys. Chem.* 92:6881–6891.
19. Hamming, R. W. 1986. Coding and Information Theory. Prentice-Hall, Englewood Cliffs, NJ.
20. Wyman, J. 1964. Linked functions and reciprocal effects in hemoglobin: a second look. *Adv. Protein Chem.* 19:223–286.
21. Di Cera, E., K-P. Hopfner, and J. Wyman. 1992. Symmetry conditions for binding processes. *Proc. Natl. Acad. Sci. USA.* 89:2727–2731.
22. Feller, W. 1950. An Introduction to Probability Theory and its Applications. Wiley, New York.
23. Spitzer, F. 1964. Principles of Random Walk. Van Nostrand, Princeton, NJ.
24. Gradshtein, S., and I. M. Ryzhik. 1980. Tables of Integrals, Series and Products. Academic, New York.

25. Niven, I., H. S. Zuckerman, and H. L. Montgomery. 1960. An Introduction to the Theory of Numbers. Wiley, New York.
26. Matthew, J. B., and F. R. N. Gurd. 1986. Calculation of electrostatic interactions in proteins. *Methods Enzymol.* 130:413–453.
27. Gilson, M. K., and B. H. Honig. 1988. Energetics of charge-charge interactions in proteins. *Proteins.* 3:32–53.
28. Bashford, D. 1991. Electrostatic interactions in biological molecules. *Curr. Opin. Struct. Biol.* 1:175–184
29. Wallace, A., S. Dennis, J. Hofsteenge, and S. R. Stone. 1989. Contribution of the N-terminal region of hirudin to its interaction with thrombin. *Biochemistry.* 28:10079–10084.
30. Betz, A., J. Hofsteenge, and S. R. Stone. 1991. Ionic interactions in the formation of the thrombin-hirudin complex. *Biochem. J.* 275:801–803.
31. Stone, S. R., and J. Hofsteenge. 1986. Kinetics of the inhibition of thrombin by hirudin. *Biochemistry.* 25:4622–4628.
32. De Cristofaro, R., J. W. Fenton, and E. Di Cera. 1992. Modulation of thrombin-hirudin interaction by specific ion effects. *J. Mol. Biol.* 226: 263–269.
33. Rydel, T. J., A. Tulinsky, W. Bode, and R. Huber. 1991. Refined structure of the hirudin-thrombin complex. *J. Mol. Biol.* 221:583–601.
34. Onsager, L. 1944. Crystal statistics. I. A two-dimensional model with an order-disorder transition. *Phys. Rev.* 65:117–128.
35. Yang, C. N., and T. D. Lee. 1952. Statistical theory of equations of state and phase transitions. I. Theory of condensation. *Phys. Rev.* 87:404–409.
36. Lee, T. D., and C. N. Yang. 1952. Statistical theory of equations of state and phase transitions. II. Lattice gas and Ising model. *Phys. Rev.* 87: 410–419.